Electronic Supplementary Material (ESI) for Journal of Materials Chemistry C.


# A study on controlling structural topologies in coordination networks: solvent-directed synthesis and distinct variations in optical properties

Zi-Xin You,[a, b†] Yao Xiao,[a†] Qing-Lin Guan,[a] Ting Zhang,[a] Yong-Heng Xing[a*] and Feng-Ying Bai [a*]

[a] *College of Chemistry and Chemical Engineering, Liaoning Normal University, Dalian City, 116029, P.R. China.*

[b] *College of Chemical Engineering, Shenyang University of Chemical Technology, Shenyang, 110142, P.R. China.*

*† The authors contribute equally to this work.*

**Content**

**Synthesis of $H_2$CMNDI:** The synthesis of ligands N,N'-bis(carboxymethyl)-1,4,5,8-naphthalimide ($H_2$CMNDI) referred to the method that reported in the previous literature. [1]

**Synthesis of Ho-CMNDI:** The synthesis method of Ho-CMNDI is similar to that of Eu-CMNDI, and the green block crystal is finally obtained. Yield: 63% (calculated based on $H_2$CMNDI). Anal. Calc. (%) for $C_{20}H_{17}N_2O_{13}Ho$: C, 36.49; H, 2.60; N, 4.26; Found (%): C, 36.54; H, 2.53; N, 4.28. ATR-IR ($cm^{-1}$): 3323 (m), 3080 (m), 1703 (s), 1660 (s), 1578 (s), 1454 (s), 1389 (s), 1351 (s), 1243 (s), 1183 (m), 1009 (m), 919 (vw), 811 (vw), 773 (s), 722 (w).

**Synthesis of Gd-CMNDI:** The synthesis method of Gd-CMNDI is similar to that of Eu-CMNDI, and the yellow block crystal is finally obtained. Yield: 65% (calculated based on $H_2$CMNDI). Anal. Calc. (%) for $C_{20}H_{17}N_2O_{13}Gd$ (%): C, 36.92; H, 2.63; N, 4.31; Found (%): C, 36.86; H, 2.61; N, 4.35. ATR-IR ($cm^{-1}$): 3218 (m), 3079 (m), 1703 (s), 1664 (s), 1573 (s), 1435 (s), 1395 (s), 1355 (s), 1245 (s), 1185 (m), 1010 (m), 917 (vw), 809 (vw), 774 (s), 724 (w).

**Synthesis of Tb-CMNDI:** The synthesis method of Tb-CMNDI is similar to that of Eu-CMNDI, and the yellow block crystal is finally obtained. Yield: 61% (calculated based on $H_2$CMNDI). Anal. Calc. (%) for $C_{20}H_{17}N_2O_{13}Tb$ (%): C, 36.83; H, 2.63; N, 4.29; Found (%): C, 36.84; H, 2.58; N, 4.35. ATR-IR ($cm^{-1}$): 3234 (m), 3079 (m), 1703 (s), 1665 (s), 1575 (s), 1436 (s), 1397 (s), 1355 (s), 1245 (s), 1185 (m), 1010 (m), 917 (vw), 809 (vw), 776 (s), 723 (w).

**Synthesis of Yb-CMNDI:** The synthesis method of Yb-CMNDI is similar to that of Eu-CMNDI, and the yellow block crystal is finally obtained. Yield: 55% (calculated based on $H_2$CMNDI). Anal. Calc. (%) for $C_{20}H_{17}N_2O_{13}Yb$ (%): C, 36.05; H, 2.57; N, 4.20; Found (%): C, 36.08; H, 2.51; N, 4.16. ATR-IR ($cm^{-1}$): 3262 (m), 3078 (m), 1703 (s), 1661 (s), 1577 (s), 1439 (s), 1394 (s), 1353 (s), 1243 (s), 1185 (m), 1009 (m), 918 (vw), 810 (vw), 773 (s), 723 (w).

**Synthesis of La-CMNDI:** The synthesis method of La-CMNDI is similar to that of Eu-CMNDI, and the yellow block crystal is finally obtained. Yield: 55% (calculated based on $H_2$CMNDI). Anal. Calc. (%) for $C_{20}H_{17}N_2O_{13}La$ (%): C, 37.99; H, 2.71; N, 4.43; Found (%): C, 38.00; H, 2.76; N, 4.38. ATR-IR ($cm^{-1}$): 3359 (m), 3085 (m), 1704 (s), 1660 (s), 1566 (s), 1430 (s), 1393 (s), 1357 (s), 1246 (s), 1187 (m), 1012 (m), 918 (vw), 809 (vw), 777 (s), 725 (w).

**Synthesis of Dy-CMNDI-F:** The synthesis method of La-CMNDI is similar to that of Tb-CMNDI-F, and the yellow block crystal is finally obtained. Yield: 60% (calculated based on $H_2$CMNDI). Anal. Calc. (%) for $C_{22}H_{16}N_3O_{11}Dy$: C, 39.98; H, 2.44; N, 6.36; Found (%): C, 39.94; H, 2.48; N, 6.36. ATR-IR ($cm^{-1}$): 3366 (m), 3084 (m), 1711 (s), 1656 (s), 1580 (s), 1437 (s), 1387 (m), 1352 (s), 1241 (s), 1182 (s), 1010 (s), 919 (vw), 809 (vw), 775 (s), 726 (w).

**Synthesis of Eu-CMNDI-F:** The synthesis method of Eu-CMNDI-F is similar to that of Tb-CMNDI-F, and the yellow block crystal is finally obtained. Yield: 57% (calculated based on $H_2$CMNDI). Anal. Calc. (%) for $C_{22}H_{16}N_3O_{11}Eu$: C, 40.63; H, 2.48; N, 6.46; Found (%): C, 40.65; H, 2.53; N, 6.50. ATR-IR ($cm^{-1}$): 3365 (m), 3083 (m), 1710 (s), 1656 (s), 1579 (s), 1434 (s), 1387 (m), 1352 (s), 1241 (s), 1182 (s), 1010 (s), 919 (vw), 809 (vw), 774 (s), 725 (w).

**Synthesis of Yb-CMNDI-F:** The synthesis method of Yb-CMNDI-F is similar to that of Tb-CMNDI-F, and the yellow block crystal is finally obtained. Yield: 58% (calculated based on $H_2$CMNDI). Anal. Calc. (%) for $C_{22}H_{16}N_3O_{11}Yb$: C, 39.35; H, 2.40; N, 6.26; Found (%): C, 39.37; H, 2.35; N, 6.30. ATR-IR ($cm^{-1}$): 3365 (m), 3084 (m), 1710 (s), 1658 (s), 1581 (s), 1440 (s), 1387 (m), 1353 (s), 1241 (s), 1182 (s), 1010 (s), 919 (vw), 809 (vw), 776 (s), 726 (w).

**Synthesis of La-CMNDI-F:** The synthesis method of La-CMNDI-F is similar to that of Tb-

CMNDI-F, and the yellow block crystal is finally obtained. Yield: 60% (calculated based on $H_2$CMNDI). Anal. Calc. (%) for $C_{22}H_{16}N_3O_{11}La$: C, 41.46; H, 2.53; N, 6.59; Found (%): C, 41.41; H, 2.51; N, 6.55. ATR-IR ($cm^{-1}$): 3365 (m), 3086 (m), 1707 (s), 1660 (s), 1579 (s), 1425 (s), 1383 (s), 1351 (s), 1242 (s), 1182 (m), 1011 (m), 918 (vw), 809 (vw), 775 (s), 725 (w).

**Synthesis of Pr-CMNDI-F:** The synthesis method of Pr-CMNDI-F is similar to that of Tb-CMNDI-F, and the yellow block crystal is finally obtained. Yield: 54% (calculated based on $H_2$CMNDI). Anal. Calc. (%) for $C_{22}H_{16}N_3O_{11}Pr$: C, 41.33; H, 2.52; N, 6.57; Found (%): C, 41.34; H, 2.57; N, 6.50. ATR-IR ($cm^{-1}$): 3365 (m), 3083 (m), 1707 (s), 1656 (s), 1579 (s), 1428 (s), 1386 (s), 1353 (s), 1241 (s), 1182 (m), 1011 (m), 918 (vw), 809 (vw), 774 (s), 726 (m).

**Synthesis of Sm-CMNDI-F:** The synthesis method of Sm-CMNDI-F is similar to that of Tb-CMNDI-F, and the yellow block crystal is finally obtained. Yield: 51% (calculated based on $H_2$CMNDI). Anal. Calc. (%) for $C_{22}H_{16}N_3O_{11}Sm$: C, 40.73; H, 2.49; N, 6.48; Found (%): C, 40.65; H, 2.51; N, 6.50. ATR-IR ($cm^{-1}$): 3366 (m), 3084 (m), 1711 (s), 1654 (s), 1580 (s), 1433 (s), 1387 (s), 1352 (s), 1241 (s), 1182 (m), 1010 (m), 919 (vw), 809 (vw), 775 (s), 725 (m).

**X-ray Crystallographic Determination**

The Bruker AXS TENSOR-27 FT-IR spectrometer was applied to record Infrared spectra in the range of 4000-400 $cm^{-1}$. UV-vis absorption spectra of solid sample were received from a JASCO V-570 UV/VIS/NIR spectrophotometer with the range of 200-800 nm, and Lambda 35 spectrometer was applied to record the UV-vis absorption spectra of suspension samples in 200-800 nm. Thermogravimetric data was obtained from a PerkinElmer Diamond TG/DTA under nitrogen protection from room temperature to 1100 °C with the heating rate of 10 °C·$min^{-1}$. X-ray powder diffraction (PXRD) patterns were performed on an Advance D8 equipped with Cu-Kα radiation in the range of $5° < 2\theta < 60°$, with a step size of 0.02° (2θ) and a count time of 2 s per step. The HORIBA Fluoromax-4-TCSPC spectrofluorometer which is provided with Pulsed LED sources (200-1000 nm) with 3.2-inch Integrating Sphere was used to measure the fluorescence behavior of the coordination complexes at room temperature. The size and morphology of the material surface was investigated by Scanning Electron Microscope & X-ray Analyzer (SEM, SU8010) and Atomic Force Microscope (AFM, Asylum Research Cypher ES). The crystallographic diffraction data of Ln-CMNDI and Ln-CMNDI-F were measured on Bruker AXS SMART APEX II CCD diffractometer graphite monochromatized Mo Kα radiation (λ = 0.71073 Å) at 293 K and were displayed in Table S1 and Table S2. The space group was determined by Olex2 platform and, all atoms were anisotropic ally refined by direct method (XL) and least-squares refinement (XS) in the final cycle. For the series of Ln-CMNDI, three crystallographic diffraction data were obtained. There are several level alerts in the checkCIF files. Therefore, we provided reasonable explanations for these alerts. For Ln-CMNDI (Ln=Eu, Gd, Ho), PLAT417_ALERT_2_B could be explained as there is no accurately modeled water hydrogen position in the structure and therefore the interatomic H-H distances calculated are likely incorrect.[2] PLAT420_ALERT_2_B could be explained as O1W-H1WB and O1W-H1WA are part of a water molecule that is likely disordered/on a partially occupied site.[3] For Gd-CMNDI, regrettably, there is an A alert and we tried to adjust the appropriate conditions but still failed to obtain a better quality crystal so we provided reasonable explanations for the alert A here. THETM01_ALERT_3_A could be explained as it is related to the crystal quality The crystal was poorly diffracting at high angle. For Ln-CMNDI-F, (Ln=Tb, Dy), PLAT430_ALERT_2_B could be explained as atoms form a hydrogen bonded network of water molecules in the pore of the framework

**Table S1** Crystallographic information of Ln-CMNDI-F*

| CNs | Tb-CMNDI-F | Dy-CMNDI-F |
|---|---|---|
| Formula | $C_{22}H_{16}N_3O_{11}Tb$ | $C_{22}H_{16}N_3O_{11}Dy$ |
| M ($g \cdot mol^{-1}$) | 657.30 | 660.88 |
| Crystal system | *Monoclinic* | *Monoclinic* |
| Space group | $P2_1/c$ | $P2_1/c$ |
| a (Å) | 9.1044(6) | 9.0936(7) |
| b (Å) | 28.345(2) | 28.333(2) |
| c (Å) | 8.3863(6) | 8.3529(6) |
| α (°) | 90 | 90 |
| β (°) | 94.7790(10) | 94.8850(10) |
| γ (°) | 90 | 90 |
| V ($Å^3$) | 2156.6(3) | 2144.3(3) |
| Z | 4 | 4 |
| $D_c$ ($g \cdot cm^{-3}$) | 2.024 | 2.047 |
| F(000) | 1288 | 1292 |
| M(Mo Kα) ($mm^{-1}$) | 3.353 | 3.559 |
| θ (°) | 2.245-31.228 | 2.248-31.199 |
| Reflections collected | 14641 | 14704 |
| Independent reflections($I>2\sigma(I)$) | 6108(4540) | 5866(4213) |
| Parameters | 336 | 336 |
| Δ(ρ)(e $Å^{-3}$) | 1.314&-1.695 | 1.463&-1.258 |
| Goodness of fit on $F^2$ | 1.060 | 1.026 |
| R[a] | 0.0325(0.0556)[b] | 0.0354(0.0624)[b] |
| $wR_2$[a] | 0.0639(0.0720)[b] | 0.0626(0.0706)[b] |

*[a]$R=\sum \left| F_O-F_C \right| / \sum \left| F_O \right|$, $wR_2=\{\sum[w(F_O^2-F_C^2)^2]/\sum[w(F_O^2)^2]\}^{1/2}$; $[F_O>4\sigma(F_O)]$. [b]Based on all data.

**Table S2** Crystallographic information of Ln-CMNDI*

| CNs | Eu-CMNDI | Ho-CMNDI | Gd-CMNDI |
|---|---|---|---|
| Formula | $C_{20}H_{17}N_2O_{13}Eu$ | $C_{20}H_{17}N_2O_{13}Ho$ | $C_{20}H_{17}N_2O_{13}Gd$ |
| M ($g \cdot mol^{-1}$) | 645.31 | 658.28 | 650.60 |
| Crystal system | *Triclinic* | *Triclinic* | *Triclinic* |
| Space group | $P\bar{1}$ | $P\bar{1}$ | $P\bar{1}$ |
| a (Å) | 9.2284(12) | 9.2901(15) | 9.2409(9) |
| b (Å) | 9.5731(12) | 9.4885(15) | 9.5443(9) |

| | | | |
|---|---|---|---|
| c (Å) | 14.0350(18) | 13.896(2) | 14.0003(13) |
| α (°) | 74.687(2) | 74.085(2) | 74.574(2) |
| β (°) | 77.477(2) | 77.350(3) | 77.472(2) |
| γ (°) | 66.129(2) | 65.475(3) | 66.097(2) |
| V (Å$^3$) | 1085.1(2) | 1063.9(3) | 1079.85(18) |
| Z | 2 | 2 | 2 |
| $D_c$ (g·cm$^{-3}$) | 1.975 | 2.055 | 2.001 |
| F(000) | 636 | 644 | 638 |
| M(Mo Kα) (mm$^{-1}$) | 2.968 | 3.798 | 3.149 |
| θ (°) | 1.516-28.986 | 1.535-30.570 | 1.521-28.282 |
| Reflections collected | 7140 | 7445 | 6941 |
| Independent reflections($I$>2σ($I$)) | 5207(4398) | 5516(4500) | 5024(3767) |
| Parameters | 328 | 331 | 331 |
| Δ(ρ)(e Å$^{-3}$) | 1.208&-0.834 | 0.971&-1.110 | 0.808&-0.906 |
| Goodness of fit on $F^2$ | 1.051 | 1.011 | 0.989 |
| R[a] | 0.0330(0.0428)[b] | 0.0358(0.0511)[b] | 0.0465(0.0741)[b] |
| $wR_2$[a] | 0.0755(0.0798)[b] | 0.0681(0.0733)[b] | 0.0830(0.0930)[b] |

*[a]$R=\sum \left| F_O-F_C \right| / \sum \left| F_O \right|$, $wR_2=\{\sum[w(F_O^2-F_C^2)^2]/\sum[w(F_O^2)^2]\}^{1/2}$; [$F_O$>4σ($F_O$)]. [b]Based on all data.

**Table S3** Systre input file and output file of **lcf** topological net

| Systre input file for the Tb-CMNDI-F |
|---|
| crystal |
| name Tb-CMNDI-F |
| cell 9.1044 28.3450 8.3863 90.000 94.779 90.000 |
| group P121/c1 |
| atom 1 4 0.62530 0.50780 0.25870 |
| edge 1 0.78480 0.25230 0.22260 |
| edge 1 0.21520 0.75230 0.27740 |
| edge 1 0.78480 0.24770 -0.27740 |
| edge 1 0.21520 0.74770 0.77740 |
| atom 2 6 0.21520 0.75230 0.27740 |
| edge 2 0.21520 0.74770 -0.22260 |
| edge 2 0.21520 0.74770 0.77740 |
| edge 2 0.37470 1.00780 0.24130 |
| edge 2 0.62530 0.50780 0.25870 |
| edge 2 0.37470 0.49220 -0.25870 |

edge 2 0.62530 0.99220 -0.24130

end

Systre output file for the Tb-CMNDI-F

Structure #1 - " Tb-CMNDI-F".

Input structure described as 3-periodic.

Given space group is P121/c1.

8 nodes and 20 edges in repeat unit as given.

Structure is not connected.

Processing components separately.

==========

Processing component 1:

dimension = 2

Input structure described as 2-periodic.

Given space group is P1.

8 nodes and 20 edges in repeat unit as given.

Ideal repeat unit smaller than given (5 vs 20 edges).

Point group has 4 elements.

2 kinds of node.

Equivalences for non-unique nodes:

V3 --> V2

V4 --> V2

V5 --> V2

V6 --> V1

V7 --> V1

V8 --> V1

Coordination sequences:

Node V1: 4 12 18 24 30 36 42 48 54 60

Node V2: 6 12 18 24 30 36 42 48 54 60

TD10 = 330

Ideal space group is p2mm.

Ideal group or setting differs from given (p2mm vs P1).

Structure is new for this run.

Relaxed cell parameters:

a = 1.72587, b = 1.00534, gamma = 90.0000

Relaxed positions:

Node V1: 0.00000 0.00000

Node V2: 0.50000 0.50000

Edges:

0.00000 0.00000 <-> 0.50000 0.50000

0.50000 0.50000 <-> 0.50000 -0.50000

Edge centers:

0.25000 0.25000

0.50000 0.00000

Edge statistics: minimum = 0.99867, maximum = 1.00534, average = 1.00000

Angle statistics: minimum = 59.77884, maximum = 180.00000, average = 111.42857

Shortest non-bonded distance = 1.00534

Degrees of freedom: 2

Finished component 1.

==========

Finished structure #1 - " Tb-CMNDI-F ".

**Table S4** Systre input file and output file of **lcn** net

| Systre input file for the Eu-CMNDI |
|---|
| crystal |
| name Eu-CMNDI |
| cell 9.2284 9.5731 14.0350 74.687 77.477 66.129 |
| group P-1 |
| atom 1 5 0.29920 0.40410 0.46960 |
| edge 1 0.26720 -0.03060 0.98790 |
| edge 1 0.26720 0.96940 -0.01210 |
| edge 1 0.73280 0.03060 0.01210 |
| edge 1 0.73280 1.03060 0.01210 |
| edge 1 -0.26720 0.03060 1.01210 |
| atom 2 7 0.73280 0.03060 0.01210 |
| edge 2 0.26720 -0.03060 -0.01210 |
| edge 2 1.26720 -0.03060 -0.01210 |
| edge 2 0.70080 -0.40410 0.53040 |
| edge 2 0.70080 0.59590 -0.46960 |
| edge 2 0.29920 0.40410 0.46960 |
| edge 2 0.29920 -0.59590 0.46960 |

edge 2 1.29920 0.40410 -0.53040

end

Systre output file for the Eu-CMNDI

Structure #1 - "Eu-CMNDI".

Input structure described as 3-periodic.

Given space group is P-1.

4 nodes and 12 edges in repeat unit as given.

Given repeat unit is accurate.

Point group has 4 elements.

2 kinds of node.

Coordination sequences:

Node 1: 5 20 43 76 119 168 231 300 379 468

Node 2: 7 20 45 76 119 170 231 300 381 468

TD10 = 1814

Ideal space group is C12/c1.

Ideal group or setting differs from given (C12/c1 vs P-1).

Structure is new for this run.

Group setting modified to A12/n1

Relaxed cell parameters:

a = 1.93283, b = 3.00966, c = 1.72982

alpha = 90.0000, beta = 116.3841, gamma = 90.0000

Cell volume: 9.01443

Relaxed positions:

Node 1: 0.25000 0.37552 0.25000

Node 2: 0.25000 0.04237 0.25000

Edges:

0.25000 0.04237 0.25000 <-> 0.75000 0.12448 0.25000

0.25000 0.04237 0.25000 <-> 0.25000 0.37552 0.25000

0.25000 0.04237 0.25000 <-> 0.25000 -0.12448 -0.25000

0.25000 0.04237 0.25000 <-> 0.75000 -0.04237 0.75000

Edge centers:

0.50000 0.08342 0.25000

0.25000 0.20895 0.25000

0.25000 -0.04105 0.00000

0.50000 -0.00000 0.50000

Edge statistics: minimum = 0.99751, maximum = 1.00268, average = 1.00000

Angle statistics: minimum = 59.76288, maximum = 151.31260, average = 102.20621

Shortest non-bonded distance = 1.22496

Degrees of freedom: 6

Finished structure #1 - "Eu-CMNDI".

**Table S5** Structural comparison of Ln-CMNDI and Ln-CMNDI-F

| CNs | Eu-CMNDI | Tb-CMNDI-F |
|---|---|---|
| Coordination environment | 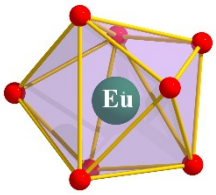  | 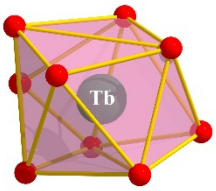  |
| Coordination number | 8 | 9 |
| Metal-$O_{carb}$ average bond length | 2.423 Å | 2.497 Å |
| Connection | 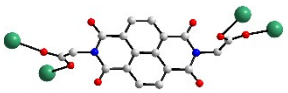 | 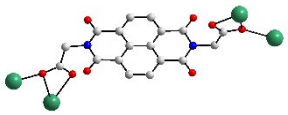 |
| Linking pattern | $\mu_4$-$\eta_O^1\eta_O^1\eta_O^1\eta_O^1$ | $\mu_4$-$\eta_O^1\eta_O^2\eta_O^1\eta_O^2$ |
| π-π interactions | 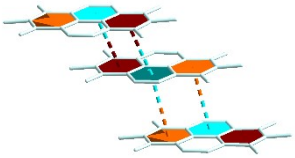 | 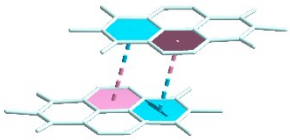 |
| Contacts between ring centroids | 3.61-3.64 Å | 3.56 Å |
| Lone pair-π interactions | 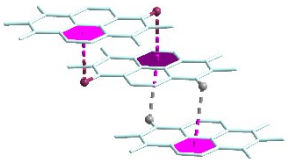 | 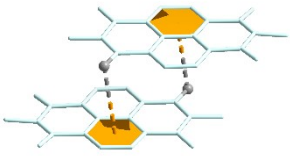 |
| Contacts of oxygen to ring centroids | 3.55-3.62 Å | 3.48 Å |
| Topological type | 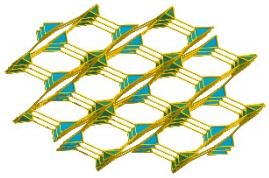 | 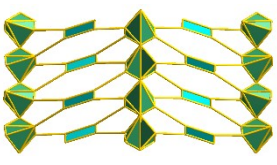 |
| RCSR symbol | **lcn** | **lcf** |

| Point symbol | $\{3^2.4^4.5^4\}\{3^4.4^6.5^6.6^5\}$ | $\{3^2.4^2.5^2\}\{3^4.4^4.5^4.6^3\}$ |
|---|---|---|

**Table S6** Average R.G.B. values of time-dependent photochromic photos

| CNs | Eu-CMNDI | Eu-CMNDI-F |
|---|---|---|
| 0 h | (175, 154, 122) | (136, 112, 78) |
| 0.5 h | (79, 69, 65) | (46, 26, 16) |
| 1 h | (63, 53, 52) | (38, 21, 14) |
| 1.5 h | (62, 52, 51) | (34, 18, 12) |
| 2 h | (59, 50, 50) | (31, 17, 13) |

**Table S7** π-π interactions in Eu-CMNDI and Tb-CMNDI-F*

| CNs | Cg(I) | Cg(J) | Cg-Cg (Å)[a] | α (°)[b] | Symmetry code(J) |
|---|---|---|---|---|---|
| Eu-CMNDI | Cg1 | Cg4 | 3.64 | 0.8(2) | 1-x, 1-y, 1-z |
| | Cg2 | Cg4 | 3.61 | 0.7(2) | -x, 1-y, 1-z |
| Tb-CMNDI-F | Cg1 | Cg3 | 3.56 | 1.41(17) | 1-x, 1-y, 1-z |

*Eu-CMNDI: Cg1: N1→C5→C7→C10→C8→C6→; Cg2: N2→C17→C15→C13→C16→C18→; Cg4: C8→C10→C13→C16→C14→C11→; Tb-CMNDI-F: Cg1: N1→C7→C9→C12→C10→C8→; Cg3: N2→C19→C17→C15→C18→C20→; [a] Cg-Cg: Distance between ring centroids of π-π interactions; [b] α: Dihedral angle between planes of π-π interactions.

**Table S8** Lone pair-π interactions in Eu-CMNDI and Tb-CMNDI-F*

| CNs | Y-X | Cg(J)[a] | X..Cg (Å)[b] | Y-X..Cg (°)[c] | Symmetry code(J) |
|---|---|---|---|---|---|
| Eu-CMNDI | C6- | Cg3 | 3.62 | 97.8(3) | 1-x, 1-y, 1-z |
| | C18- | Cg3 | 3.55 | 99.6(3) | -x, 1-y, 1-z |
| Tb-CMNDI-F | C8- | Cg2 | 3.48 | 92.3(2) | 1-x, 1-y, 1-z |

*Eu-CMNDI: Cg3: C7→C9→C12→C15→C13→C10→; Tb-CMNDI-F: Cg2: C9→C11→C14→C17→C15→C12→; [a] Cg(J) = Center of gravity of ring J; [b] X..Cg = Distance of X to Cg; [c] Y-X..Cg = Y-X-Cg angle

**Table S9** Comparison of quenching effect constants of Ln-CNs on nitrophenols and literature level*

| Material | $K_{SV(PNP)}$ /$M^{-1}$ | $K_{SV(DNP)}$ /$M^{-1}$ | $K_{SV(TNP)}$ /$M^{-1}$ | Ref. |
|---|---|---|---|---|
| $CeO_2$/ZnO | $6.38\times10^3$ | n.a. | n.a. | [144] |
| MOPs **II** | $1.69\times10^4$ | n.a. | n.a. | [143] |
| Complex **4** | $4.9\times10^3$ | n.a. | n.a. | [153] |
| Zn-ddn | n.a. | $8.93\times10^3$ | n.a. | [160] |
| HPU-12 | n.a. | $3.07\times10^4$ | n.a. | [161] |
| LZn | n.a. | $1.54\times10^4$ | $1.62\times10^4$ | [162] |
| LCd | n.a. | $1.39\times10^4$ | $1.56\times10^4$ | [162] |
| Zn-MOF | n.a. | n.a. | $2.40\times10^4$ | [163] |

| | | | | |
|---|---|---|---|---|
| EuBr | n.a. | n.a. | $1.70\times10^4$ | [164] |
| TbBr | n.a. | n.a. | $2.02\times10^4$ | [164] |
| **Eu-CMNDI** | **$2.92\times10^3$** | **$5.07\times10^4$** | **$2.31\times10^4$** | **this work** |
| **Eu-CMNDI-F** | **$3.25\times10^3$** | **$3.80\times10^4$** | **$1.92\times10^4$** | **this work** |

**Table S10** Comparison of limit of detection of Ln-CNs towards nitrophenols and literature level*

| Material | $LOD_{(PNP)}$ /μM | $LOD_{(DNP)}$ /μM | $LOD_{(TNP)}$ /μM | Ref. |
|---|---|---|---|---|
| $CeO_2$/ZnO | 3.05 | n.a. | n.a. | [144] |
| AuNPs@PDA | 6.30 | n.a. | n.a. | [145] |
| MOPs **II** | 1.46 | n.a. | n.a. | [143] |
| HPU-12 | n.a. | 8490 | n.a. | [161] |
| LZn | n.a. | 53.0 | 50.4 | [162] |
| LCd | n.a. | 46.6 | 41.5 | [162] |
| JLU-MOF201-Tb | n.a. | 2.29 | n.a. | [158] |
| M-TMU-58 | n.a. | n.a. | 6 | [159] |
| EuBr | n.a. | n.a. | 10 | [164] |
| TbBr | n.a. | n.a. | 10 | [164] |
| **Eu-CMNDI** | **6.25** | **0.36** | **0.79** | **this work** |
| **Eu-CMNDI-F** | **8.75** | **0.75** | **1.48** | **this work** |

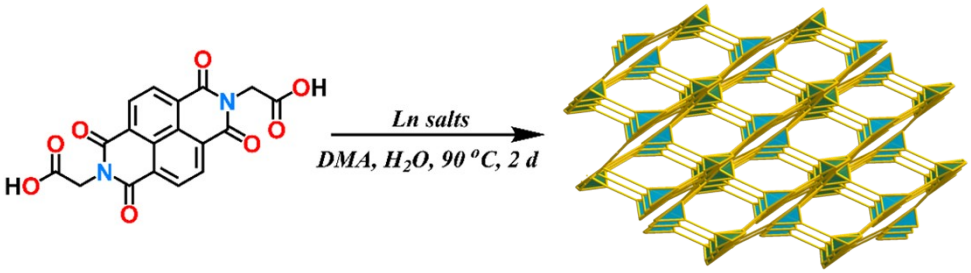


**Scheme S1** Schematic diagram of Ln-CMNDI synthesis process

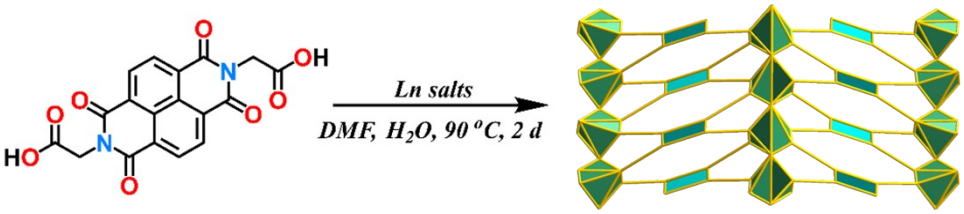


**Scheme S2** Schematic diagram of Ln-CMNDI-F synthesis process

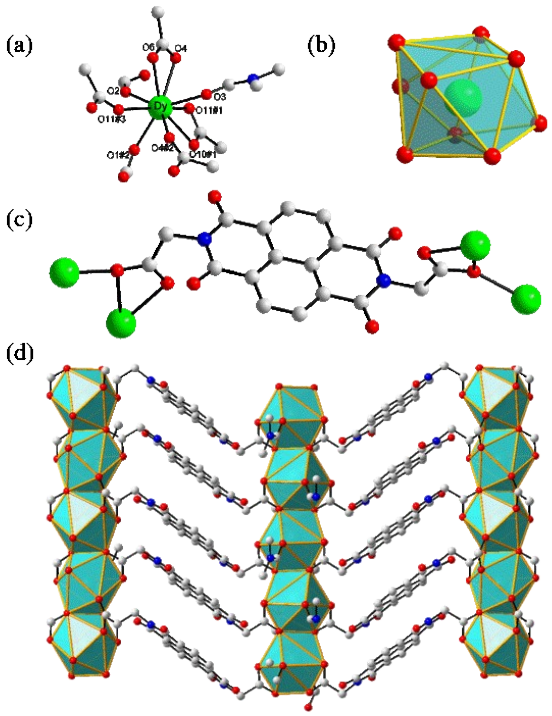


**Figure S1** Structure of Dy-CMNDI-F: (a) Coordination environment of Co(II) (#1 -x+1, -y+2, -z; #2 -x+1, -y+1, -z+1; #3 x+1, y+1, z-1); (b) Spatial configuration of a Tb–O polyhedron; (c) Connection of CMNDI; (d) 2D network

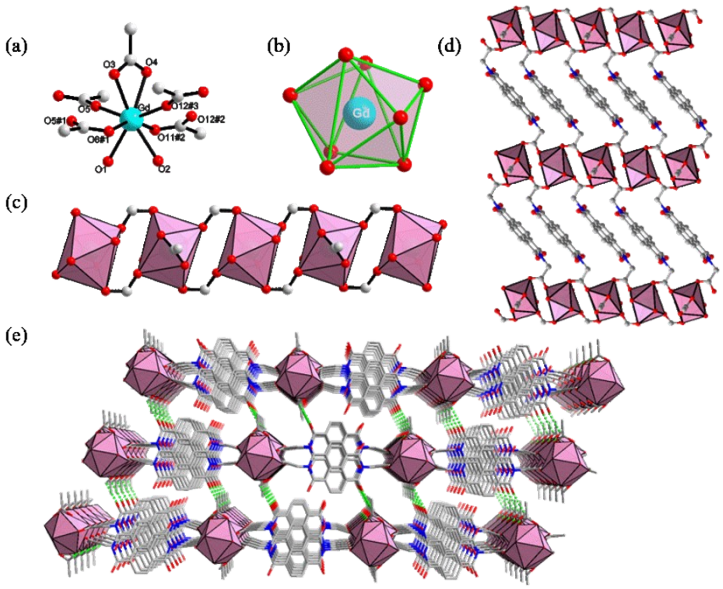


**Figure S2** structure of Gd-CMNDI: (a) Coordination environment of Gd(III) (#1 -x+1, -y+2, -z; #2 -x+1, -y+1, -z+1; #3 x+1, y+1, z-1); (b) Spatial configuration of an Gd–O polyhedron; (c) Connection of CMNDI; (d) 2D network; (e) 3D supramolecular network

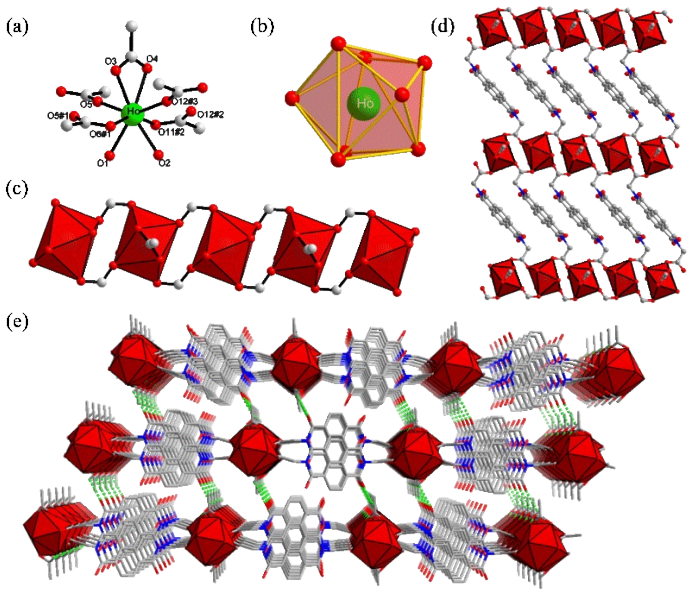


**Figure S3** structure of Ho-CMNDI: (a) Coordination environment of Ho(III) (#1 -x+1, -y+2, -z; #2 -x+1, -y+1, -z+1; #3 x+1, y+1, z-1); (b) Spatial configuration of an Ho–O polyhedron; (c) Connection of CMNDI; (d) 2D network; (e) 3D supramolecular network

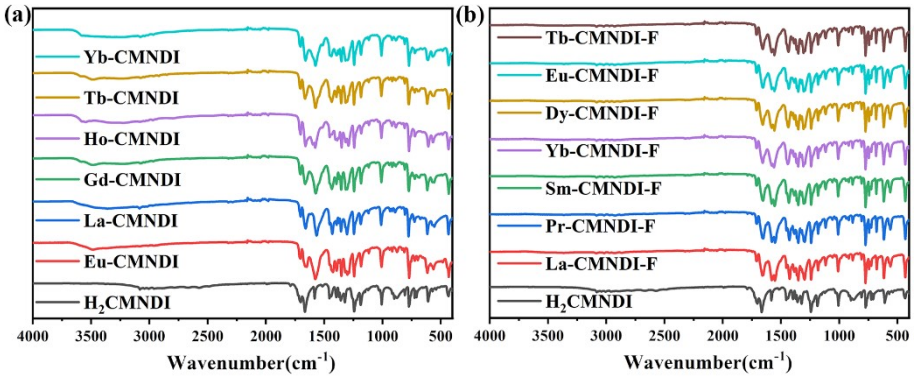


**Figure S4** ATR-IR spectra of $H_2$CMNDI, Ln-CMNDI and Ln-CMNDI-F

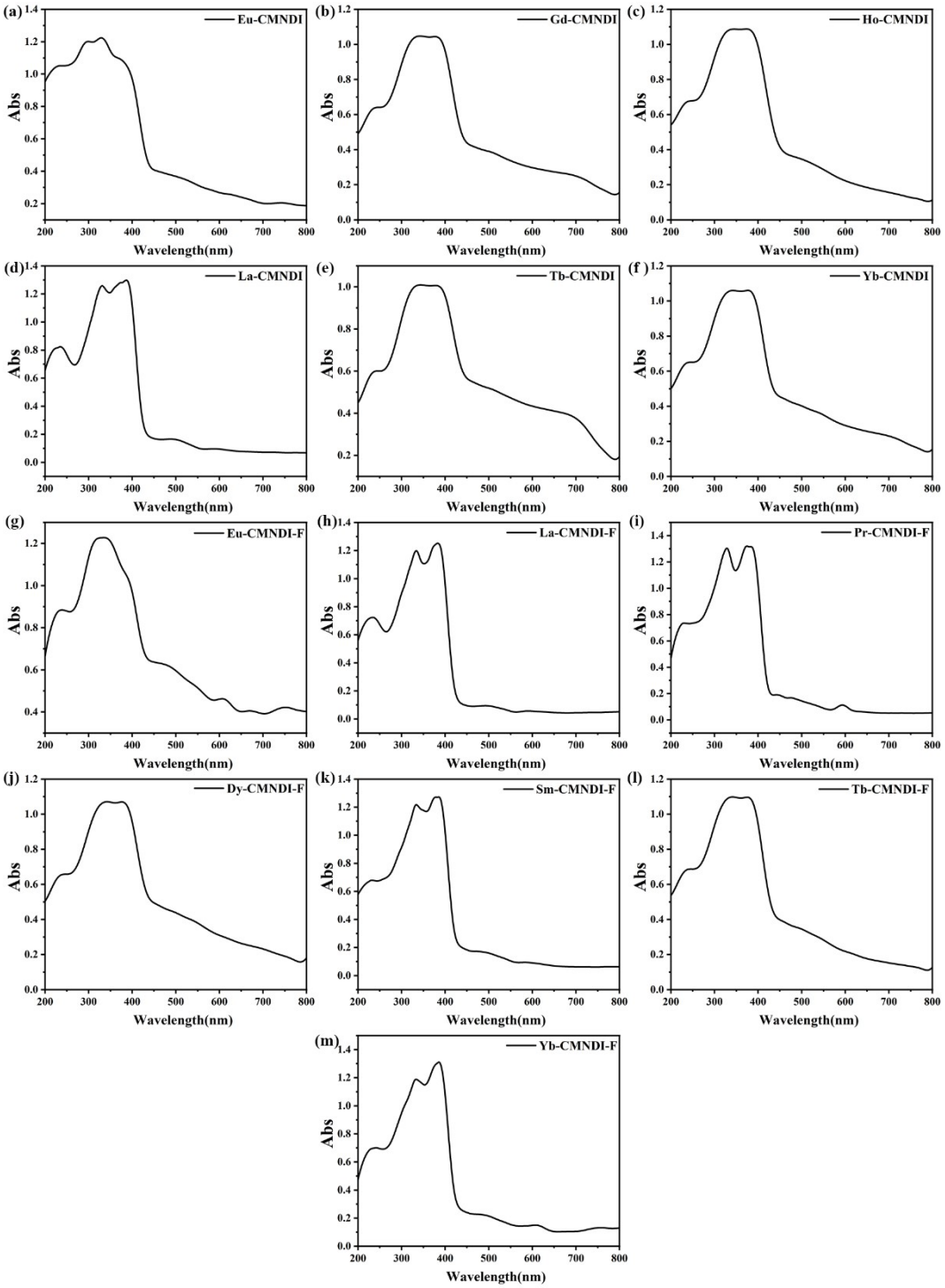


**Figure S5** UV-vis spectra of Ln-CMNDI and Ln-CMNDI-F

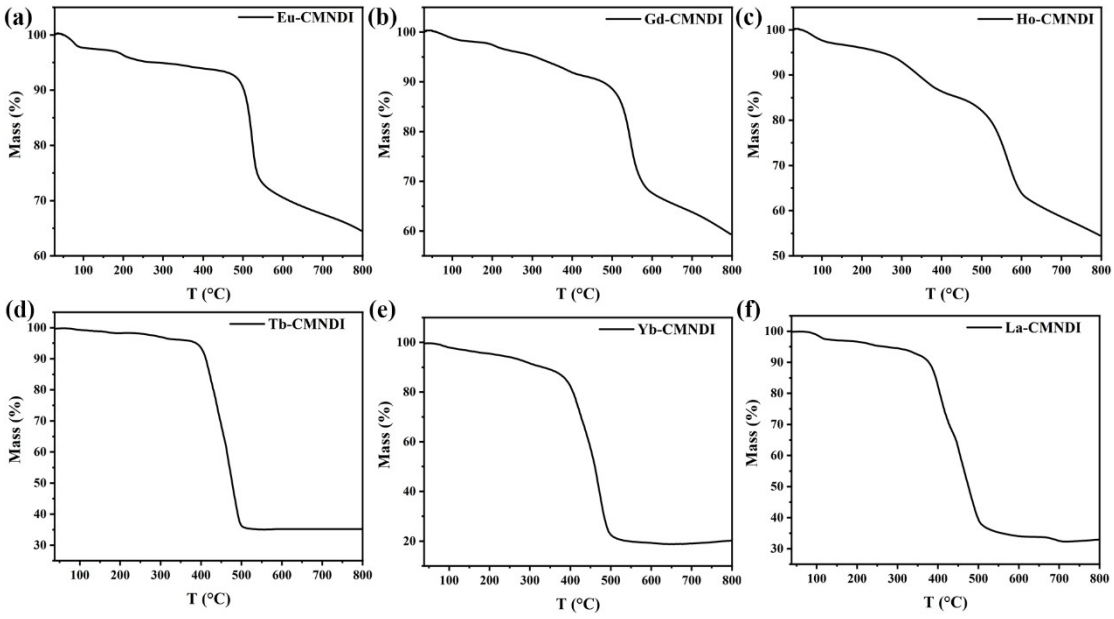


**Figure S6** TG curves in $N_2$ atmosphere of Ln-CMNDI

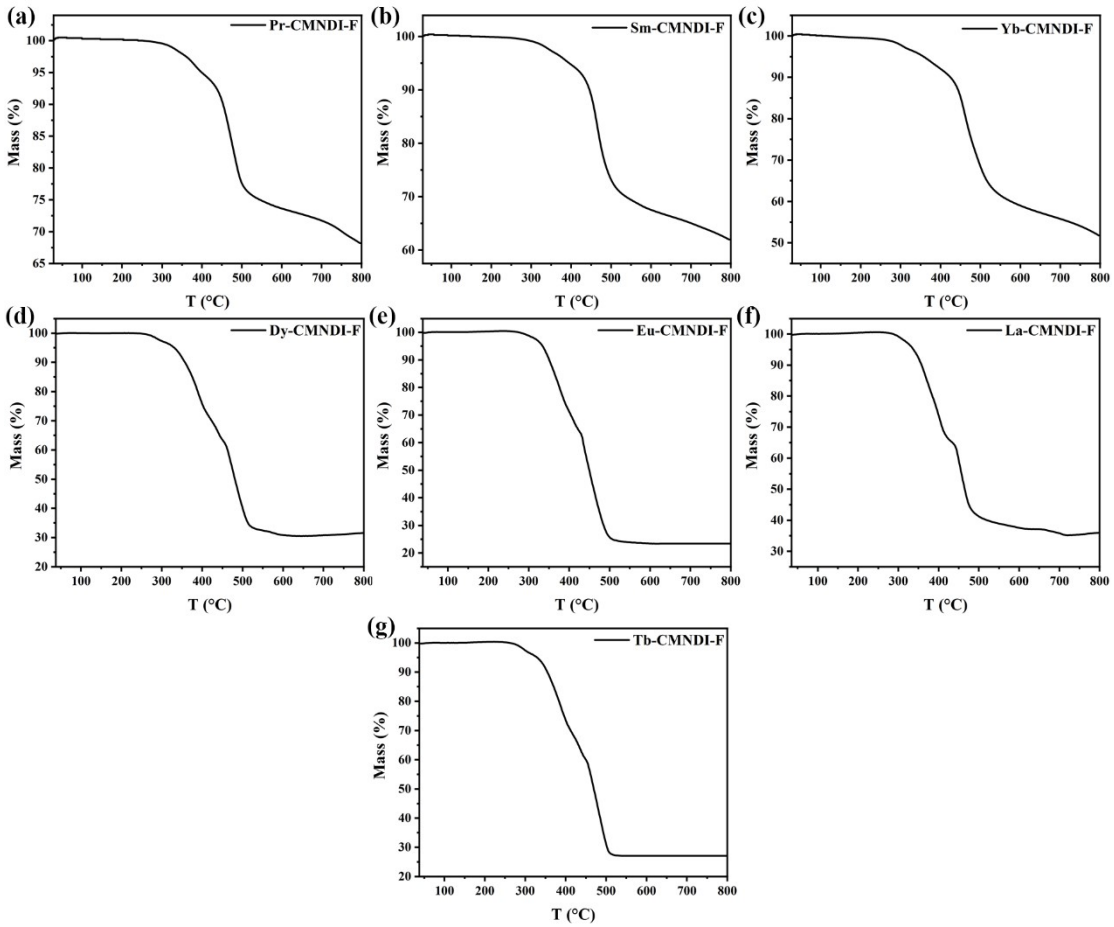


**Figure S7** TG curves in $N_2$ atmosphere of Ln-CMNDI-F

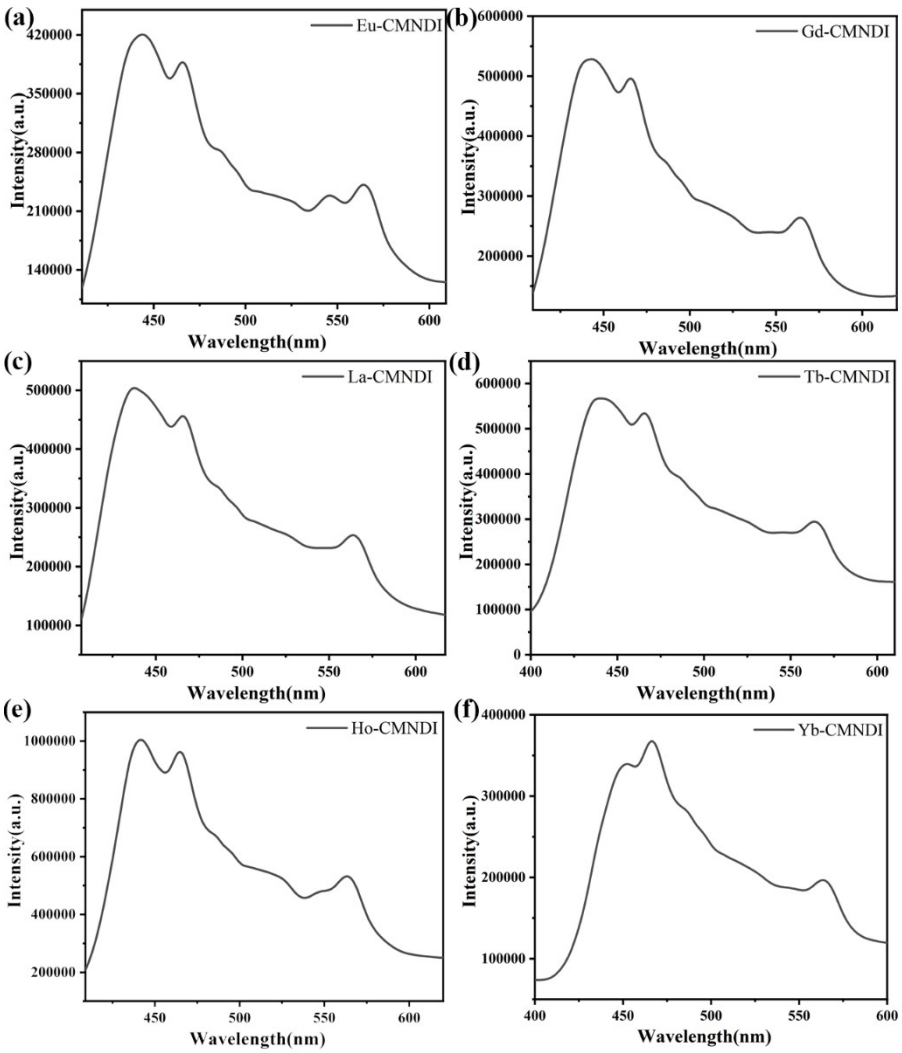


**Figure S8** The solid state fluorescence spectra of Ln-CMNDI

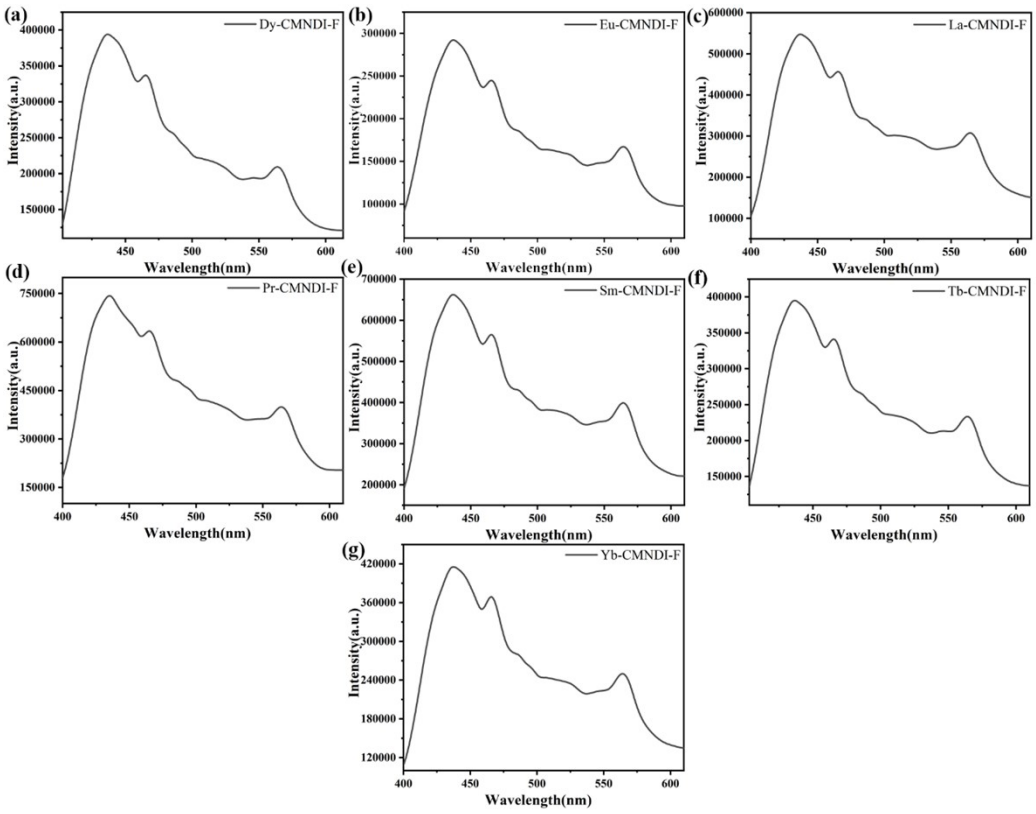


**Figure S9** The solid-state fluorescence spectra of Ln-CMNDI-F

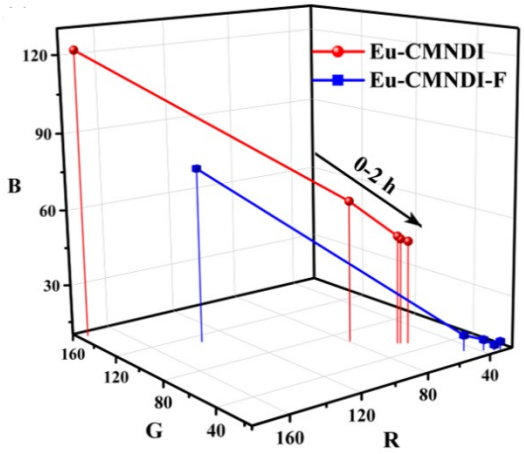


**Figure S10** R.G.B. value change of Eu-CMNDI and Eu-CMNDI-F under ultraviolet irradiation

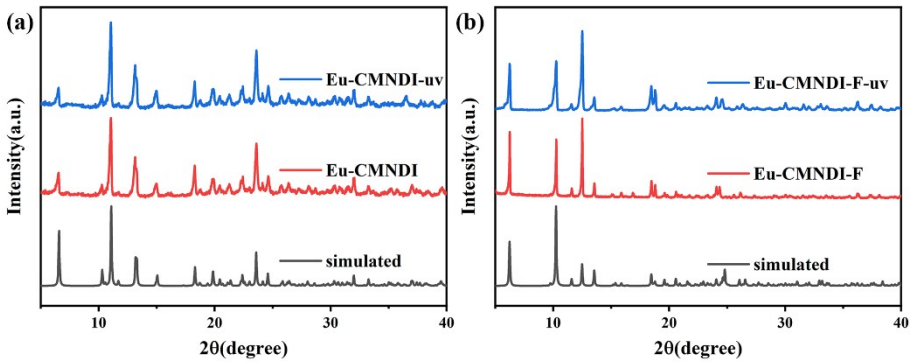


**Figure S11** The PXRD patterns of Eu-CMNDI (a) and Eu-CMNDI-F (b) which were simulated, experimental, and after UV irradiation

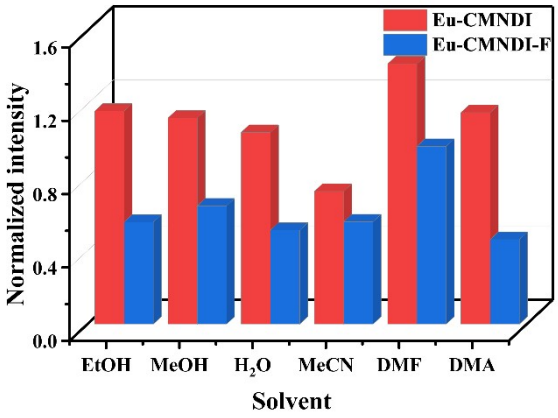


**Figure S12** The fluorescence intensity of Eu-CMNDI and Eu-CMNDI-F in different solvents

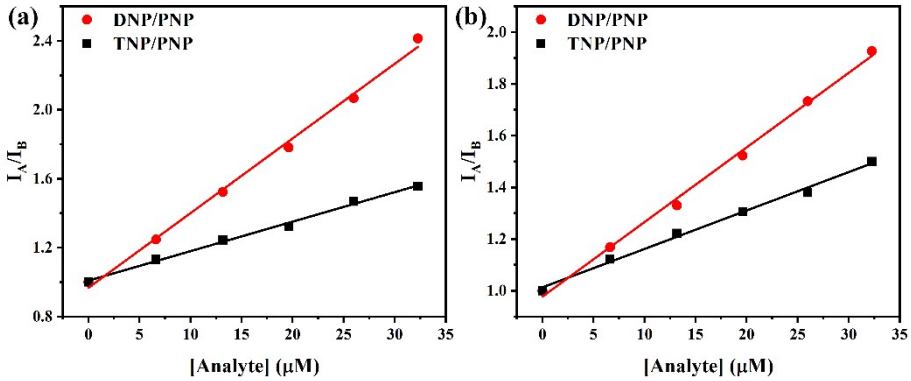


**Figure S13** Quenching recognition constant plots of (a) Eu-CMNDI and (b) Eu-CMNDI-F for recognition of mono- and poly-nitrophenols

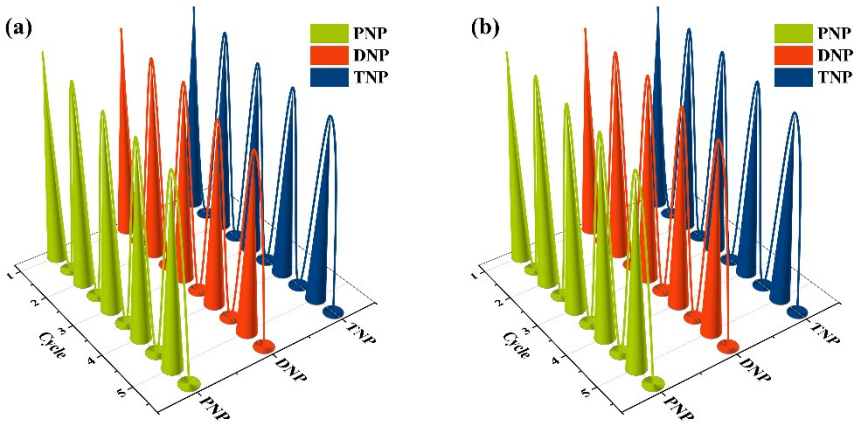


**Figure S14** The cycle experiment of (a) Eu-CMNDI and (b) Eu-CMNDI-F

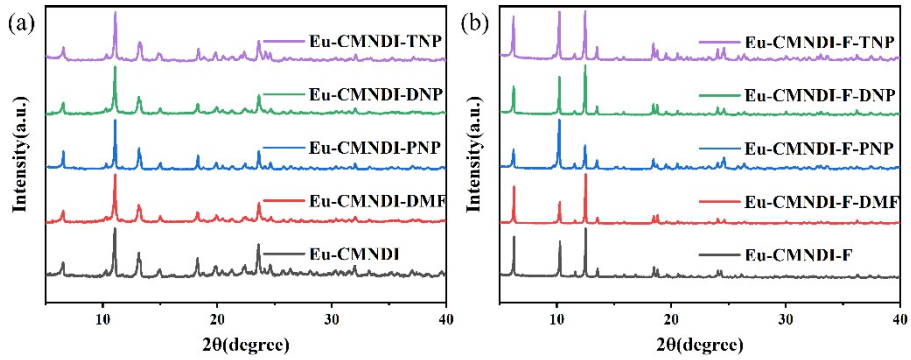


**Figure S15** PXRD patterns of Eu-CMNDI (a) and Eu-CMNDI-F (b) before and after sensing nitrophenols

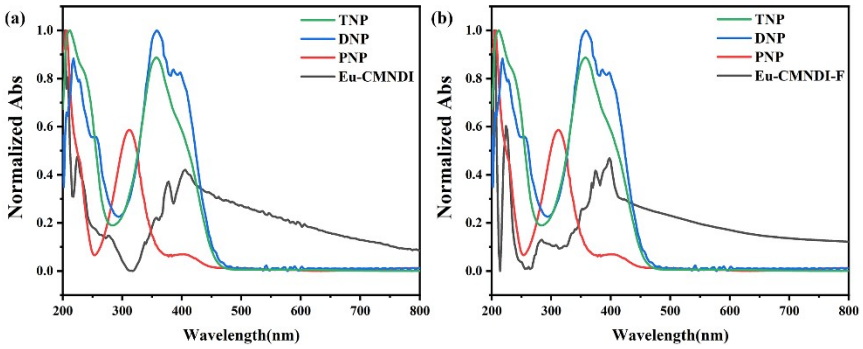


**Figure S16** Overlap of absorption spectra of Eu-CMNDI (a), Eu-CMNDI-F (b), and nitrophenols

**Reference**


1. H. Y. Au-Yeung, F. B. L. Cougnon, S. Otto, G. D. Pantoş and J. K. M. Sanders, Exploiting donor–acceptor interactions in aqueous dynamic combinatorial libraries: exploratory studies of simple systems, *Chem Sci*, 2010, **1**, 567-574.
2. A. J. Dennington and M. T. Weller, Synthesis and structure of pseudo-three dimensional hybrid iodobismuthate semiconductors, *Dalton T*, 2016, **45**, 17974-17979.
3. L. K. Saunders, H. Nowell, H. C. E. Spencer, L. E. Hatcher, H. J. Shepherd, L. H. Thomas, C. L. Jones, S. J. Teat, P. R. Raithby and C. C. Wilson, Tuning charge-assisted and weak hydrogen bonds in molecular complexes of the proton sponge DMAN by acid co-former substitution, *CrystEngComm*, 2018, **20**, 3074-3083.
4. B. Laramée-Milette and G. S. Hanan, Going against the flow: Os(II)-to-Ru(II) energy transfer in rod-like polypyridyl chromophore, *Chem Commun*, 2017, **53**, 10496-10499.
5. J. Binns, K. V. Kamenev, K. E. R. Marriott, G. J. McIntyre, S. A. Moggach, M. Murrie and S. Parsons, A non-topological mechanism for negative linear compressibility, *Chem Commun*, 2016, **52**, 7486-7489.